Available online at www.sciencedirect.com
ScienceDirect
Ceramics International 35 (2009) 2735–2740
CERAMICS INTERNATIONAL
www.elsevier.com/locate/ceramint

Fracture behaviour of Mg-PSZ ceramics: Comparative estimates

George A. Gogotsi *

Pisarenko Institute for Problems of Strength, 2, Timiryazevskaya Str., 01014 Kiev, Ukraine

Received 1 December 2008; received in revised form 9 February 2009; accepted 3 March 2009
Available online 27 March 2009

Abstract

The mechanical behaviour of different Mg-PSZ ceramics is studied. Results of their edge fracture (EF) and single edge V-notch beam (SEVNB) tests are discussed. These inelastic ceramics exhibit nonlinear relations between the fracture load and the distance from the extreme point on the chip scar to the specimen edge. They also possess nonlinearly rising R-lines. It is established that the data points plotted in the EF base diagram fall below the baseline (lower barrier to the onset of fracture). By projecting these data points onto the baseline, fracture toughness values close to those of the matrix are determined. The limitations of conventional procedures for evaluating the mechanical behaviour of these ceramics were found out. It has been demonstrated that the EF test method can be quite adequate for enhancing the reliability of comparative fracture resistance estimates.

Keywords: C. Fracture; Toughness and toughening; D. ZrO_2; Indentation; Edge flaking (chipping)

1. Introduction

For a long time ZrO_2 was used only in the manufacture of refractory ceramics designed for thermal insulation. However, this material had considerable promise, which provided further incentive to studies on its mechanical behaviour. It was established that the ability of cubic zirconia-based refractory ceramics to resist fracture under mechanical and thermal loadings can increase with the content of the monoclinic phase [1]. This effect arises from the introduction of microcracks into the structure of the material, i.e., one of the mechanisms is realized, which fostered development of toughened zirconia ceramics [2]. Interest in structural zirconia ceramics has quickened after a publication devoted to Ceramic steel [3], where it was shown that the stress-induced martensitic transformation of metastable tetragonal particles of this material to a stable monoclinic phase was a mechanism, which absorbs energy and inhibits crack propagation.

Though considerable resources and much effort were spent for the investigation and development of the above ceramics, their use has not become as extensive as first expected. It can also be explained by the fact that their mechanical behaviour was treated almost in the same way as that of the conventional ceramics (or steel) without considering the specific features of this transformation-toughened and inelastic material. All this leads to estimates that are not reliable enough.

The above gave impetus to the investigation, which became the object of the present communication. Basic experiments made use of the SEVNB method [4], built upon the linear fracture mechanics concepts [5], and the edge fracture (EF) test method [6,7] that provides direct estimation (not corrected by any calculation models) of the fracture resistance of brittle materials.

2. Materials and methods

2.1. Ceramics

The goal of the present investigation was to gain an understanding of the fracture behaviour of Mg-PSZ ceramics. Therefore, the experiments were based on their representative versions (Table 1), studied earlier. These materials were supplied by ICI Advanced Ceramics (Australia) for making joint studies (comparative tests to check performance of our procedures was carried out on TS-grade ceramics [8]). The specimens of TS and MS ceramics [9], TSE and TSN ceramics, containing 25 and 70% of the monoclinic phase [10] (12% in TS), as well as of SF-S-MS ceramics [6], annealed for another 1 h when compared to normal conditions, were taken as the basic objects of investigation. In addition, SF-S-TS ceramics

* Tel.: +380 44 285 44 64; fax: +380 44 286 16 84.
E-mail address: ggogotsi@ipp.kiev.ua.

0272-8842/$36.00 © 2009 Published by Elsevier Ltd and Techna Group S.r.l.
doi:10.1016/j.ceramint.2009.03.007

Table 1
Mechanical characteristics of ceramics.

Material	Brittleness measure χ	Elastic modulus (GPa)	Strength (MPa)	Fracture toughness (SEVNB) (MPa $m^{1/2}$)	Fracture toughness (SENB) (MPa $m^{1/2}$)
TS	0.58	198	632	9.12 ± 0.14	9.67 ± 0.24
MS	0.83	187	654	6.92 ± 0.26	9.18 ± 0.65
TSE	0.89	207	563	4.88 ± 0.12	6.82 ± 0.27
TSN	0.65	162	160	4.03 ± 0.22	4.02 ± 0.22
SF-S-MS	0.56	201	600	9.50 ± 0.20	11.38 ± 0.26
SF-S-TS	0.93	193	236	5.13 ± 0.14	7.18 ± 0.19
Y-TZP	1.00	211	774	5.34 ± 0.65	7.83 ± 0.67

were tested, they were annealed for further 12 h in comparison with SF-S-MS ceramics. All these materials were produced from the same powders by similar sintering technology, but their annealing that followed sintering was specific in each case (for theoretical grounds see [9]), which altered their mechanical characteristics, including fracture toughness. Comparative tests were performed on Y-TZP ceramics [11] (Table 1).

2.2. Test procedures

At the first stage of investigations, tests in four-point flexure (20 mm/40 mm span sizes) of 4 mm × 5 mm cross-section rectangular specimens were carried out with a CeramTest device (Gobor Ltd., Ukraine), mounted on a universal test machine [12]. As a result, load–deflection curves (deformation diagrams) were plotted and used for determining the strength and static elastic moduli (stress–strain relation covering the initial portion of the deformation diagram) as for estimating inelasticity. The latter is characterized by the brittleness measure χ [13], equal to the ratio of the specific elastic energy, accumulated in the specimen to the moment of fracture, to the specific energy, spent for its deformation by the same moment (for elastic ceramics $\chi = 1$). The next step was to study the behaviour of these ceramics under thermal shock loading by a procedure [14]. By this test, 5 mm × 5 mm cross-section bars were heated in an electric furnace and then quenched in a water bath at room temperature. After that their residual strength was determined in four-point flexure. The results were presented as furnace-water bath temperature difference ΔT–residual strength σ relations (thermal shock resistance diagrams). Then Vickers indentations of polished specimens were performed to analyze the fracture behaviour of these ceramics under local loading. After this, the fracture toughness of ceramics was evaluated by the SEVNB method [4]. In the specimen prepared for the tests, a 200-μm prenotch (served as a stress concentrator for SENB tests) was cut out with a diamond saw, and then it was filled with a 1–2-μm diamond paste that was distributed with a reciprocating razor, which provided polishing out a V-notch. The V-notch sharpness was measured as a circle diameter inscribed in the notch tip. In these experiments 3 mm × 4 mm-cross-section ground bars 23–25 mm long were fractured on a CeramTest device with a loading support for three-point flexure. Fracture toughness values, obtained by the SEVNB and SENB procedures, were calculated by the formula usually used for this purpose [15].

Further alternative tests were performed by the EF test method [6,7], when the rectangular specimen edge was flaked off with a Rockwell C-Scale standard conical diamond indenter of a 200-μm tip radius (Gilmore Diamond Tools, Inc., USA). The indentation point near the specimen edge was chosen with a magnifying glass, the fracture load P_f being registered by PC. Then the fracture distance L from the extreme point of the chip scar to the specimen edge was measured on an Olympus 51MX binocular microscope (Fig. 1a).

In Rockwell indentations a Hertzian ring crack (primary crack) was first formed near the specimen edge. This is well seen in glass tests (Fig. 1b). From this crack a conical crack started growing deep into the specimen. But due to the distortion of the stress field in this zone, associated with an increase in the material compliance as the indenter is approached the side (open) surface of the specimen, this crack acquired the shape of a quasi-cone, which can be observed in

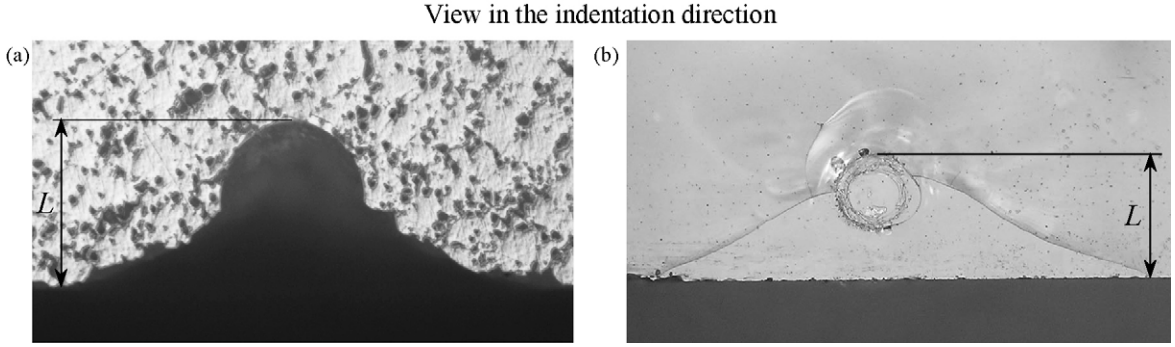

Fig. 1. Chip scar on the specimen edge of TSN ceramics (Nomarski interference) (a) and Hertzian ring crack near the edge of a fused silica specimen (b): P_f and L for (a) 54 N and 0.22 mm, for (b) 265 N and 0.44 mm, respectively.

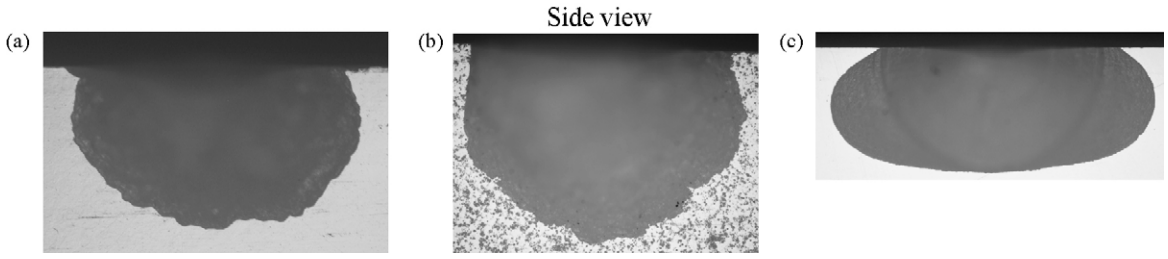

Fig. 2. Chip scars on SF-S-TS (a), TSN (b), and Y-TZP (c) specimens: P_f and L for (a) 238 N and 0.35 mm, for (b) 155 N and 0.45 mm, for (c) 106 N and 0.18 mm, respectively.

the experiments with glasses [16]. However, especially for coarse-grained ceramics, chip scars were deformed (Fig. 2). These experiments usually made use of polished specimen fragments after fracture toughness tests, with their edge radii not exceeding 20 μm. The tests were also carried out on a CeramTest device, but the loading support was replaced with the X-Y table and indenter holder. The accuracy of the specimen surface position relative to a moving indenter was of great importance. Therefore, the specimens were glued to photographic glasses with Loctite Super Glue (Henkel Corp.) and clamped on the X-Y table. The test results were used to calculate the fracture resistance F_R [6] as a ratio of the fracture load P_f to the fracture distance L and to plot P_f–L relations (fracture diagrams) approximated by the straight lines, their slope factor E_t [7] was considered as an additional characteristic of the fracture resistance. Then F_R–L relations, termed R-lines [6], were also plotted.

3. Results and discussion

Mechanical characteristics of Mg-PSZ ceramics are summarized in Table 1. Their deformation diagrams as well as thermal shock resistance diagrams are shown in Fig. 3. Fracture diagrams and R-lines are presented in Fig. 4. Since indentation points on the specimen edge are chosen arbitrarily and fracture resistance values for examined materials are

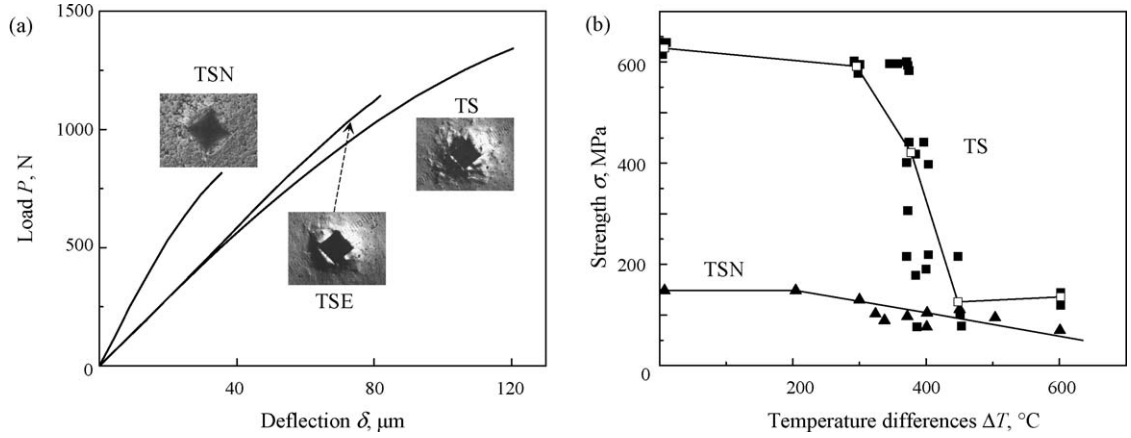

Fig. 3. Deformation diagrams with Vickers impressions (Nomarski interference) on TSN, TSE, and TS specimens (a) and thermal shock resistance diagrams (b).

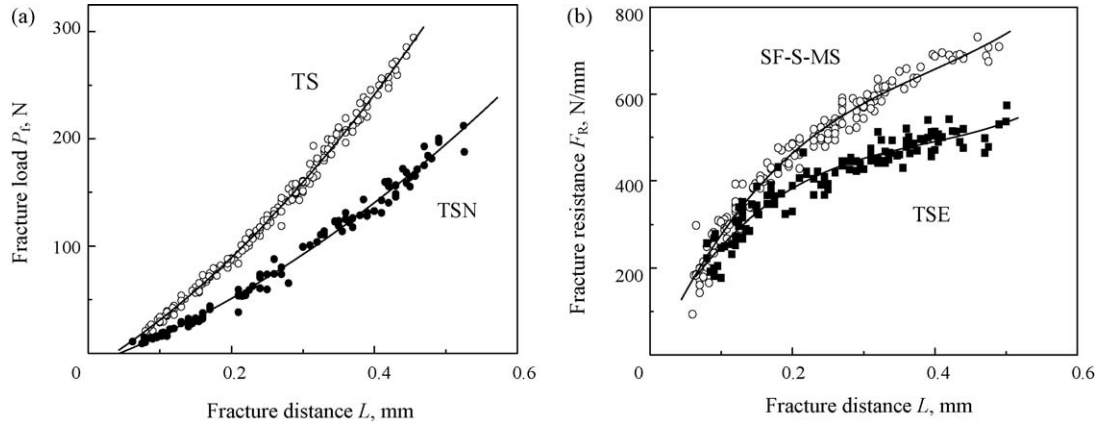

Fig. 4. Fracture diagrams (a) and R-lines (b).

Table 2
Results of EF tests.

Material	Fracture resistance (N/mm)			E_t (N/mm)	K_z (MPa m$^{1/2}$)
	F_R [a]	F_{Rmax}	F_{Rz}		
TS	483 ± 95 (175)	617 (23)	404 (24)	707	4.13
MS	455 ± 68 (165)[b]	601 (19)	397 (51)	709	4.10
TSE	403 ± 94 (121)	503 (18)	334 (24)	586	3.37
TSN	281 ± 81 (100)	368 (25)	215 (17)	434	2.25
SF-S-MS	464 ± 15 (157)	693 (13)	383 (20)	779	4.06
SF-S-TS	438 ± 93 (183)	552 (17)	353 (34)	658	3.60
Y-TZP	582 ± 100 (139)	662 (15)	–	745	–

[a] F_R and E_t correspond to the whole data body, F_{Rmax} is the average value for L = 0.40–0.50 mm.
[b] (number of chips).

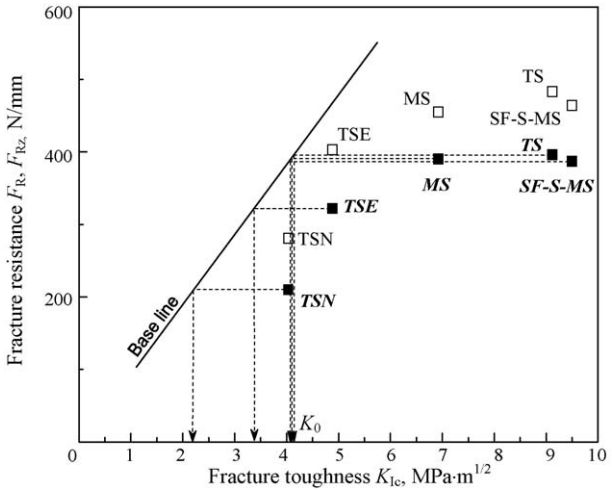

Fig. 5. EF base diagram for examined ceramics and their K_z estimates: data points for F_R (□) and F_{Rz} (■).

influenced by crack lengths (Table 2), analysis of EF test results made use not all experimental data but only those that correspond to the same fracture distances L.

As is seen in Fig. 3a and Table 1, all these ceramics are inelastic materials. Vickers impressions reveal differences in phase transformation zones on the specimen surfaces (Fig. 3a). The behaviour of these materials is different under thermal shock loading (Fig. 3b), much like that revealed in their tests on hollow cylindrical specimens [10]. The K_{Ic} estimates (Table 1) show distinctly that these ceramics differ considerably in their ability to resist fracture. The EF tests of examined ceramics resulted in nonlinear fracture diagrams and nonlinearly rising R-lines (Fig. 4). Such a line for TS-grade ceramics [6] was compared with the R-curve [5] of the same material [17]. The results of this investigation do not contradict a general view of Mg-PSZ ceramics, they contribute to better understanding of the mechanical behaviour of examined materials and corroborate the reliability of employed experimental procedures.

Detailed analysis of test data would be interesting to start with comparison of fracture resistance values obtained by the test procedures. Fracture toughness (K_{Ic}) and fracture resistance (F_{Rmax}) values for the same Mg-PSZ ceramics (Tables 1 and 2) reveal similarity of the two estimates. Those estimates vary in much the same manner when specimens are additionally annealed (SF-S-TS and SF-S-MS ceramics) or monoclinic phase contents are changed (TS, TSE, and TSN ceramics). The above lends support to the suitability of the EF test method for comparative evaluation of the fracture behaviour of Mg-PSZ ceramics.

Having knowledge of K_{Ic} and F_R values for examined ceramics, it would be adequate to plot test results (data points) in the EF base diagram (Fig. 5), these points (Table 2) fall below the baseline. Thus, Mg-PSZ ceramics exhibit a lower resistance to the onset of fracture inherent in their surface layers, as compared to ceramics having data points corresponding to the baseline (this effect is also typical of particulate ceramic composites [6,18]). Analysis of R-lines (Fig. 4b) demonstrates that they are different-sloped nonlinear-rising, approximated by the third-degree polynomial, and within these experiments they do not reach the fracture resistance plateau. This distinguishes the examined ceramics from similar tough but elastic Y-TZP ceramics, which possess F_R values, approaching maximum ones, over an examined range of fracture distances L, i.e., their R-line starts reaching plateau (Fig. 6). The difference may be explained by transformation zones present in these materials [19]. At the same time, R-lines of conventional elastic ceramics and glasses, i.e., materials that do not posses the R-curve effect, are straight, differently sloped in the F_R-L diagram [6]. Thus, the results confirm the conclusion [6] that nonlinearly rising R-lines demonstrate the relationship between the fracture resistance of Mg-PSZ ceramics and crack sizes, i.e., they display the R-curve effect.

The portions of the R-lines corresponding to the fracture distances $L \approx 125$–175 μm may be considered as their specific zones, denoted by A in Fig. 7, their origins coincide with the onset of secondary chip cracks on the specimen edge. Those cracks lengthen with indentation loads (Fig. 7b). Fracture resistance values for these zones, designated as F_{Rz}, are similar for TS, MS, and SF-S-MS ceramics (Table 2). This is probably a fracture zone, where mechanisms, responsible for the arrest of a crack formed in the process of specimen edge flaking, are still not involved. After this zone, R-lines start fanning out, with

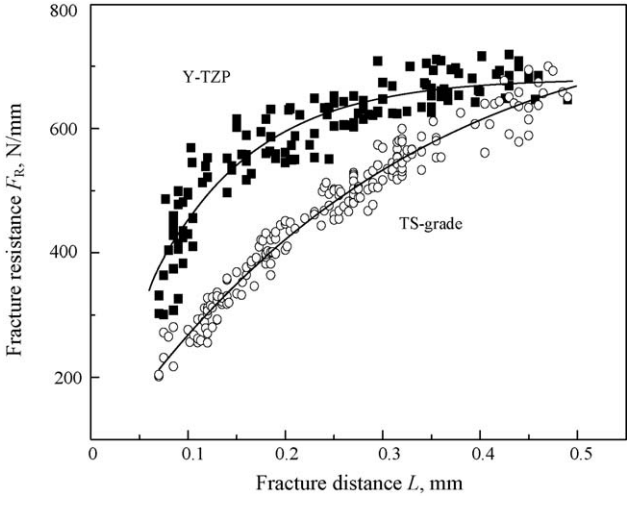

Fig. 6. R-lines for Y-TZP and TS-grade ceramics.

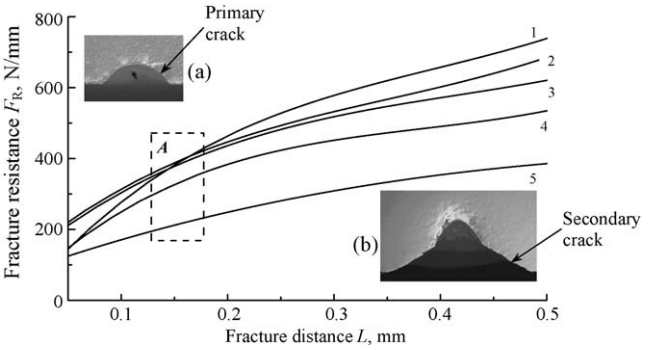

Fig. 7. Chip scars, corresponding to the initial (a) and final (b) R-line portions for SF-S-MS ceramics (Nomarski interference), R-lines for SF-S-MS (1), TS (2), MS (3), TSE (4), TSN (5) ceramics and their A zone: P_f and L for (a) 16.4 N and 0.065 mm, for (b) 336.4 N and 0.46 mm.

their slopes being the steeper, the higher the fracture toughness K_{Ic} (and fracture resistance F_R). A similar effect was found out during the examination of R-curves for the same materials [20]: $K_R(\Delta a) = K_0 + \Delta K_c(\Delta a)$, where K_0 is the fracture toughness of the matrix (fracture resistance of the material in the transformation zone immediately ahead of the crack tip [2]), Δa is the crack length, and $\Delta K_c(\Delta a)$ describes the ability of the material to resist crack propagation.

By projecting F_{Rz} values for MS, TS, and SF-S-MS ceramics onto the baseline (Fig. 5), K_z values are determined (Table 2). They turned out to be almost equal to numerical fracture toughness values of the matrix (K_0), e.g., 4 MPa $m^{1/2}$ for AF ceramics [21], their versions being used to prepare examined ceramics. For similar Mg-PSZ ceramics, containing up to 38–44% of the monoclinic phase, K_0 = 3 MPa $m^{1/2}$ [22], i.e., their K_0 values hold an intermediate position with respect to TSE and TSN ceramics (Fig. 5). The fracture toughness K_z can vary during aging, which is well seen when comparing SF-S-MS and SF-S-TS test results. This refers equally to fracture toughness values of the matrix [2]. From the above, one may suggest that K_z can be used on a par with K_0 for characterizing the ability of the material to resist fracture before the onset of crack propagation. Therefore, the K_z value can be looked on as an additional characteristic of ceramics, which is also suitable for more accurate evaluation of the initial portion of the R-curve [23].

In the first approximation, the difference in R-line slopes for examined ceramics is considered the same as of their R-curves [6]. In materials science research, when the fact of the existing relationship between fracture resistance and crack lengths (R-curve effect) is of importance for understanding the behaviour of the material, the role of R-curves and R-lines is probably the same, but the latter are obtained incomparably simpler and would require much smaller test material quantities.

Having the above information, the remark in the Introduction can be formulated more precisely. If fracture toughness estimates are critically evaluated, it should be kept in mind that they are based on the linear fracture mechanics concepts [5] (standards for testing the fracture resistance of ceramics are also built on these principles, e.g., [15]). Thus, examined materials are modeled by the linear elastic and isotropic solid of linear fracture mechanics, on the assumption that large plastic (inelastic) deformation may exist close to the crack but does not extend away from the crack by more than a small fraction of the crack length [24]. One should also assume that the rising R-curve effect (fracture resistance – crack length relationship) is nonexistent, since its presence makes it impossible to characterize the material by a single fracture toughness value [5]. Those facts are not usually taken into consideration. However [25], the absence of linearity at large strains would require the use of J-integral rather than K_{Ic}. In other words, the evaluation of Mg-PSZ ceramics should be based not only on the linear fracture mechanics concepts but also on the elastic-plastic fracture mechanics principles. Thus, one should not ignore the mechanical behaviour of these materials when estimating their fracture resistance. With the account of the above, our (and of other authors) fracture toughness values cannot probably be considered reliable estimates of the true fracture resistance of examined ceramics and may be suitable only for comparative estimates of their fracture behaviour. Similar outcomes are also referred to the reliability of strength estimates of Mg-PSZ ceramics in flexure, which are usually performed in accordance with the elasticity theory concepts.[1] Hence, these final conclusions should be interpreted as open to discussion.

4. Conclusions

Modern approaches to determining fracture toughness characteristics of Mg-PSZ ceramics have been critically analyzed. It has been demonstrated that on the basis of results, e.g., obtained in SEVNB and EF tests, they exhibit fracture resistance values that are close enough, and any significant differences in their R-curve and R-line slopes are not observed. Therefore, for technology jobs it is sufficient to evaluate their F_R and K_z values as well as to analyze their R-lines, which can be performed in a conventional materials science laboratory with small-size specimens. Detailed studies on the fracture behaviour of ceramics and comparison of their properties with published data would require determining the fracture toughness K_{Ic} and studying R-curves.

Acknowledgements

Ceramics for the experiments were kindly presented by ICI Advanced Ceramics (Australia), by Prof. M. Swain (The University of Sydney, Australia) and Dr. G. Quinn (NIST, USA). The author is thankful to V. Galenko, T. Khristevich, and B. Ozersky (Pisarenko Institute for Problems of Strength, Ukraine) for their assistance in the performance of investigations.

[1] This phenomenon was examined, e.g., on the specimens of TS-grade ceramics [8]. It was found that calculations by the conventional formula resulted in a strength value of 640 MPa (assuming this material to be linear elastic), while this value was 526 MPa (considering its inelasticity).

References

[1] A.G. Gashchenko, G.A. Gogotsi, A.G. Karaulov, I.N. Rudak, Thermal shock resistance and mechanical characterization of materials based on zirconia dioxide, Strength Mater. 6 (1974) 732–736.

[2] A.G. Evans, R.M. Cannon, Toughening of brittle solids by martensitic transformations, Acta Metal. 34 (1986) 761–780.

[3] R.C. Garvie, R.H.J. Hannink, R.T. Pascoe, Ceramic steel? Nature 258 (1975) 703–704.

[4] G.A. Gogotsi, Fracture toughness of ceramics and ceramic composites, Ceram. Int. 29 (2003) 777–784.

[5] T. Anderson, Fracture Mechanics: Fundamentals and Application, second ed., CRC Press, Boca Raton, 1995.

[6] G.A. Gogotsi, Fracture resistance of ceramics: base diagram and R-line, Strength Mater. 38 (2006) 261–270.

[7] G.A. Gogotsi, S. Mudrik, V. Galenko, Evaluation of fracture resistance of ceramics: Edge fracture tests, Ceram. Int. 33 (2007) 315–320.

[8] G.A. Gogotsi, M. Swain, J. Davis, Partially stabilized ZrO_2 and its behavior under load, Refractories 1 (1991) 2–5 (in Russian).

[9] R.H.J. Hannink, P.M. Kelly, B.C. Muddle, Transformation toughening in zirconia-containing ceramics, J. Am. Ceram. Soc. 83 (2000) 461–487.

[10] G.A. Gogotsi, V.I. Galenko, V.P. Zavada, M.V. Swain, Influence of heating rate on the thermal strain induced fracture of Mg-PSZ samples, in: G. Schneider, G. Petzow (Eds.), Thermal Shock and Thermal Fatigue Behavior of Advanced Ceramics, Kluwer Academic Publishers, Netherlands, 1993, pp. 293–305.

[11] J. Kübler, Fracture toughness of ceramics using the SEVNB method, Round Robin VAMAS Report No.37/ ESIS Document D2-99, EMPA, Swiss Federal Laboratories for Materials Testing and Research, Dubendorf, Switzerland, September 1999.

[12] G.A. Gogotsi, Deformation behavior of ceramics, J. Eur. Ceram. Soc. 7 (1991) 87–92.

[13] G.A. Gogotsi, The use of brittleness measure (χ) to represent mechanical behaviour of ceramics, Ceram. Int. 15 (1989) 127–129.

[14] G.A. Gogotsi, Festigkeitsprobleme von keramischen Werkstoffen, Silikattechnik 39 (1986) 25–28.

[15] ISO 23146, Fine ceramics (advanced ceramics, advanced technical ceramics) – Test methods for fracture toughness of monolithic ceramics – Single-edge V-notch beam (SEVNB) method, ISO, Switzerland, 2008.

[16] G.A. Gogotsi, S. Mudrik, Fracture barrier estimation by the edge fracture test method, Ceram. Int. (2009), doi:10.1016/j.ceramint.2008.10.026.

[17] A.D. Drozdov, V.O. Galenko, G.A. Gogotsi, M.V. Swain, Acoustic emission during micro- and macrocrack growth in Mg-PSZ, J. Am. Ceram. Soc. 74 (1991) 1922–1927.

[18] G.A. Gogotsi, Mechanical behaviour of a silicon nitride particulate ceramic composite, Ceram. Int. 35 (2009) 1109–1114.

[19] M.V. Swain, Toughening mechanisms for ceramics, Mater. Forum 13 (1989) 237–253.

[20] I.M. Low, Critical conditions in zirconia transformation toughening, in: C. Sorrell, D. Ben-Niesen (Eds.), Materials Science Forum, Trans. Tech. Publications Ltd., Switzerland, 1988, pp. 102–109.

[21] R.J. Hannink, C.J. Howard, E.H. Kisi, M.V. Swain, Relationship between fracture toughness and phase assemblage in Mg-PSZ, J. Am. Ceram. Soc. 77 (1994) 571–579.

[22] P.F. Becher, M.V. Swain, M.K. Faber, Relation of transformation temperature to the fracture toughness of transformation-toughened ceramics, J. Mater. Sci. 22 (1987) 76–84.

[23] G.A. Gogotsi, Flaking toughness of advanced ceramics: ancient principle revived in modern times, Mater. Res. Inn. 10–2 (2006) 179–186.

[24] G.R. Irvin, Analysis of stress and strain near the end of a crack traversing a plate, Appl. Mech. 24 (1955) 361–364.

[25] A.G. Evans, K.T. Faber, Crack-growth resistance of microcracking brittle materials, J. Am. Ceram. Soc. 67 (1984) 255–260.